

A Novel Dynamic Power Controller Based VSC-HVDC Line for Power Evacuation from Independent Power Producer

Geetha R S*, Ravishankar Deekshit* and Ghamandi Lal**

This paper presents the analysis of a Voltage Source Converter based HVDC (VSC-HVDC) system applied for evacuation of power from a medium size Independent Power Producer (IPP) with a contractual requirement that a minimum quantum of the installed capacity is to be transmitted to the permission granting agency's grid substation. The balance power could be sold by the IPP to any other customer through open access power transmission. In the system considered, at sending end, AC power is supplied from the IPP to a DC line and also to an AC line. The DC line transmits pre-defined amount of power (equal to 60% of net power available after auxiliary consumption) to the agency's grid substation and the AC line facilitates transmission under open access. The AC line is connected to the central grid's substation. At the receiving end, the agency's grid substation is interconnected to the central grid substation through another AC line. For such a transmission system requirement, a high degree of control is necessary and VSC-HVDC technology emerges as a suitable option. In this paper, a detailed simulation of power flow controllability using a novel active power controller under different generation levels of IPP is carried out and the results are presented.

Keywords: Independent Power Producer, Power evacuation, VSC-HVDC, Dynamic power controller.

1.0 INTRODUCTION

For more than 100 years, HVAC transmission has been regarded as the natural choice for electrical power transmission. High Voltage DC transmission (HVDC) has been used as an alternative method for large amount of bulk power point-to-point transmission over long distances or interconnection of asynchronous grids [1]. HVDC systems and Flexible AC Transmission Systems (FACTS) increase transmission capacity and system stability in an efficient way [2-4]. However, VSC-HVDC transmission system is now emerging as a robust and economically feasible solution for power transmission. It offers a superior solution for a number of reliability and stability issues. VSC-HVDC transmission systems use pulse width modulated VSCs with inherent

voltage controlling capability. Some of the other advantages of using VSC-HVDC transmission system are: environmental benefits and economy over long distances. It is well suited to many essential applications, such as for supplying power to offshore platforms, connecting offshore wind farms to mainland grids, providing city infeeds and powering islands. VSC-HVDC can be used for back-to-back, point-to point or multi-terminal systems and for independent control of active and reactive power[5]. The application of VSC-HVDC for enhancing reliability and efficiency of the power transmission systems has been the area of interest in the recent past. The need of the hybrid AC/DC grid structure and the operational benefits of embedded VSC-HVDC system in meshed ac networks for modern power system is discussed in [6][7]. It is shown that,

*Department of EEE, BMS College of Engineering, Bangalore - 560019, India. E-mail : rsgeetha.eee@bmsce.ac.in, hod.eee@bmsce.ac.in

** Electronics Division, BHEL, Bangalore - 560026, India. E-mail: ghamandilal@bheledn.co.in

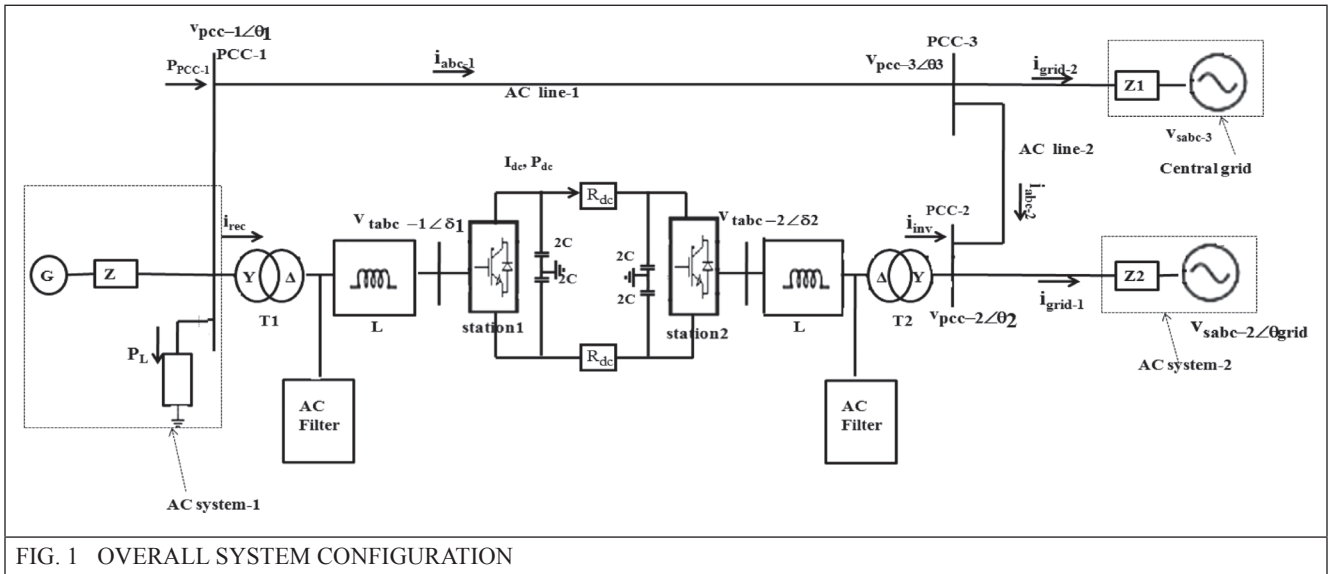


FIG. 1 OVERALL SYSTEM CONFIGURATION

embedded VSC-HVDC applications, together with the wide area measurement system, in meshed AC grids could significantly improve overall system performance, enabling smart operation of transmission grids with improved security and efficiency. In [8], through the case study of a four machine, two area network connected by VSC-HVDC, it is shown that, the transient instability of the system is prevented by the instant power reversal ability of the VSC-HVDC system. The other case studies considered in the paper suggest that, the VSC-HVDC can be used to damp ac system low frequency oscillations by active power modulation and reactive power modulation. In [9], analysis of coupling effects on overhead VSC-HVDC transmission lines from AC lines with shared Right of Way is carried out. A Hybrid Multi-Infeed HVDC System is considered in [10][11], which is a promising power transmission structure in the modern power systems. The hybrid system includes the line commutated converter (LCC) HVDC and the VSC-HVDC link.

In this paper, a dynamic power controller is proposed for power evacuation from an IPP's generating station using a VSC-HVDC system. The system chosen is shown in Figure 1. It consists of a VSC-HVDC link and AC transmission line (AC line-1) connected to the same PCC (PCC-1), which is connected to the generating station of an IPP. The other end of the VSC-HVDC link is connected to the substation of permitting

agency's substation (PCC-2), and the other end of the AC line is connected to the substation of the central grid (PCC-3). PCC-2 and PCC-3 are interconnected through another AC line (AC line-2).

In Figure 1, station-1 is a rectifier and station-2 is an inverter, and they are connected to AC system through phase reactor (L) with an internal resistance of 'R' Ω and converter transformers (T1 and T2). The two converters are linked through a DC transmission line. The phase reactors smoothen the current and secure the power exchange between AC system and DC link. The capacitors (2C) are used for voltage support and harmonic attenuation.

The other parameters of Figure 1 are as follows:

$v_{PCC-1} \angle \theta_1$: Phase voltage at PCC-1

$v_{PCC-2} \angle \theta_2$: Phase voltage at PCC-2.

$v_{PCC-3} \angle \theta_3$: Phase voltage at PCC-3

i_{abc-1} : Three phase current in AC line-1

i_{abc-2} : Three phase current in AC line-2

i_{rec} : Three phase ac current to rectifier transformer (T1)

i_{inv} : Three phase ac current output from inverter transformer (T1)

i_{grid-1} : Three phase ac current in AC system-2.

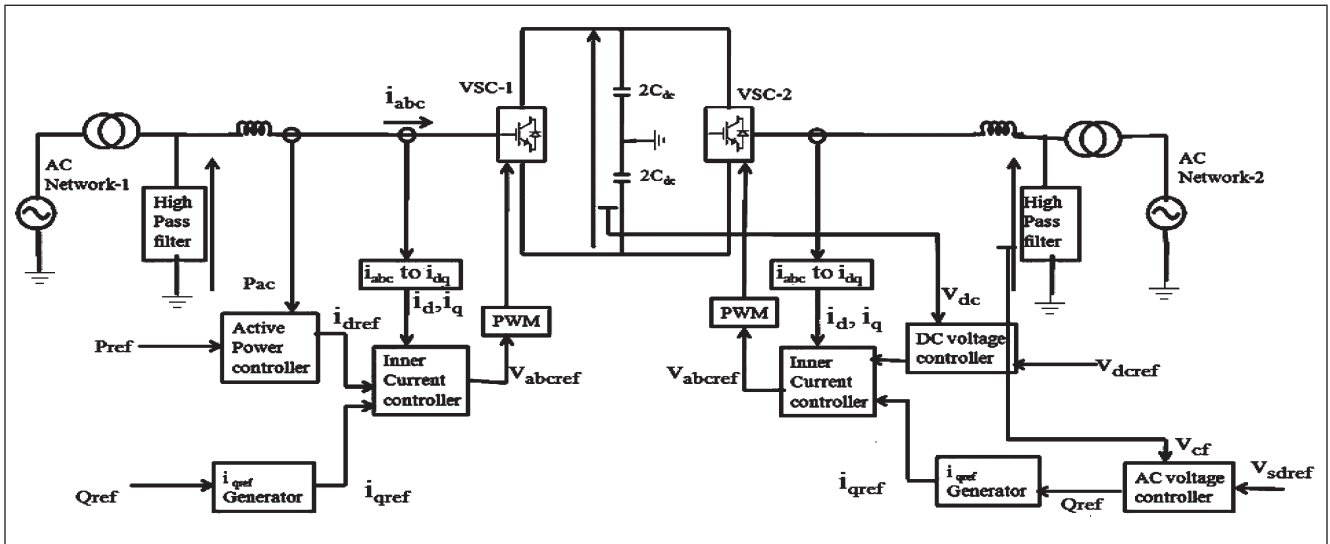


FIG. 2 BLOCK DIAGRAM OF CONTROL STRATEGIES FOR VSC_HVDC

- V_{tabc-1} : The rectifier input ac voltage
- V_{tabc-2} : The inverter output ac voltage
- P_{PCC-1} : Total active power from IPP's generating station
- P_L : The local load in IPP's generating station
- V_{dc} , I_{dc} and P_{dc} : DC voltage, DC current and DC power of VSC-HVDC system.

For the system considered, as the power transferred through the DC link is to be restricted to less than or equal to 300MW, a VSC-HVDC link is proposed. To ensure transfer of DC power under such constraints, a dynamic power controller is required to be designed. In this paper, a logic for the DC power control is proposed to ensure dynamic power transfer over VSC-HVDC link. The robustness of the controllers is tested for various power levels in the IPP's substation.

The remaining part of the paper is structured as follows: Section 2.0 discusses the control structure of the VSC-HVDC system. In section 3.0, the steady state performance analysis for case studies based on different power levels at PCC-1 is carried out.

- The results are presented for:
1. Analysis based on system parameters
 2. Analysis based on controller parameters

Conclusion drawn from the work carried out is presented in Section 4.0.

2.0 CONTROLLERS

The control scheme that has been developed for this work is aimed at the following:

1. To maintain active power that is less than or equal to 300MW in the DC link. This is achieved by implementing an Active power controller in the rectifier side of the DC link.
2. To maintain constant voltage at PCC-1 through reactive power exchange between the VSC-1 and AC system-1. A reactive power controller is used in the rectifier side for this purpose.
3. To maintain constant DC link voltage at the inverter input terminals by using a DC voltage controller.
4. To maintain constant AC voltage at the inverter output by using an AC voltage controller.

Figure 2 shows the block diagram of the overall VSC-HVDC system with different controllers. Basically, in this control scheme, the actual current in the reactor, i.e., i_{abc} is controlled using a dq reference frame through a inner current controller. The input to the inner current controllers is provided by the active power controller, reactive power controller, DC voltage controller and AC voltage controller.

The inner loop is tuned according to “Modulus optimum tuning method” [12]. The outer DC voltage loop is tuned according to “Symmetrical Optimum tuning method” [13][14]. The various controllers used in this work are explained in detail in the following section.

2.1 Inner current controller

Basically, in this control scheme, the actual current in the reactor, i.e., i_{abc} is controlled using a dq reference frame through a inner current controller. It is found in the literature that, the controller is realized by comparing the i_{dref} with i_d and the error current is passed through a PI controller to get the voltage drop (u_d) across the reactor. i_{dref} , as shown in Figure 2 is the output of the power controller, limited between the i_{dref} maximum value and i_{dref} minimum value of 0 and 1.1pu respectively.

In the following section, the governing equations for developing the current controller for inverter mode of operation (station-2) are presented. Similar equations can be developed for rectifier station. The basic equation describing the system behaviour for the inverter mode of operation is given by equation (1).

$$v_{tabc2} = Ri_{sabc2} + L \frac{di_{sabc2}}{dt} + v_{pcc-2} \quad \dots(1)$$

Transforming equation (1) to dq frame,

$$v_{tdinv} = u_{sdinv} - L\omega i_{sqinv} + v_{sdpcc-2} \quad \dots(2)$$

$$v_{tqinv} = L \frac{di_{tqinv}}{dt} + Ri_{sqinv} + L\omega i_{sdinv} + v_{sqpcc-2} \quad \dots(3)$$

;where, u_{sdinv} is given by

$$u_{sdinv} = L \frac{di_{sdinv}}{dt} + Ri_{sdinv} = [(Ls + R)i_{sdinv}] \quad \dots(4)$$

where, $v_{sdpcc-2}$, $v_{sqpcc-2}$ are the d and q components of ac voltage v_{pcc-2} , u_{sdinv} is the d component of the voltage drop across the phase reactor, i_{sdinv} , i_{sqinv} are the d and q component of the inverter ac current i_{inv} .

2.2 Active power controller

The active power (P_{ac}) is expressed in d and q components of the voltage and current [15], and is given by equation (5). In steady state, $v_{sq} = 0$ and hence, P_{ac} is given by equation (6).

$$P_{ac}(t) = \frac{3}{2} [v_{sd}(t)i_{sd}(t) + v_{sq}(t)i_{sq}(t)] \quad \dots(5)$$

$$P_{ac}(t) = \frac{3}{2} [v_{sd}(t)i_{sd}(t)] \quad \dots(6)$$

A closed loop control is used for controlling the active power. In the control methodology, the actual power P_{ac} is compared with the power to be transmitted (P_{ref}), and the error is passed through a simple PI controller. The active component of the reference current (i_{dref}) for the inner current controller is derived from this PI controller. In this paper, a new methodology for setting the value of P_{ref} under steady state condition is proposed. For the system under consideration, P_{ref} is not set at the maximum DC power (300MW) constantly. It depends on the power available in the IPP's generating station. According to the logic developed, if the generated power is less than 330 MW, (considering a local load equal to 10% of generated power), then P_{ref} is set to a value that is equal to $(P_{pcc-1} - P_L)$, which is less than 300 MW. Otherwise it is set to a value slightly greater than 300 MW owing to the DC line transmission losses. The logic used in setting P_{ref} is represented in Figure 3.

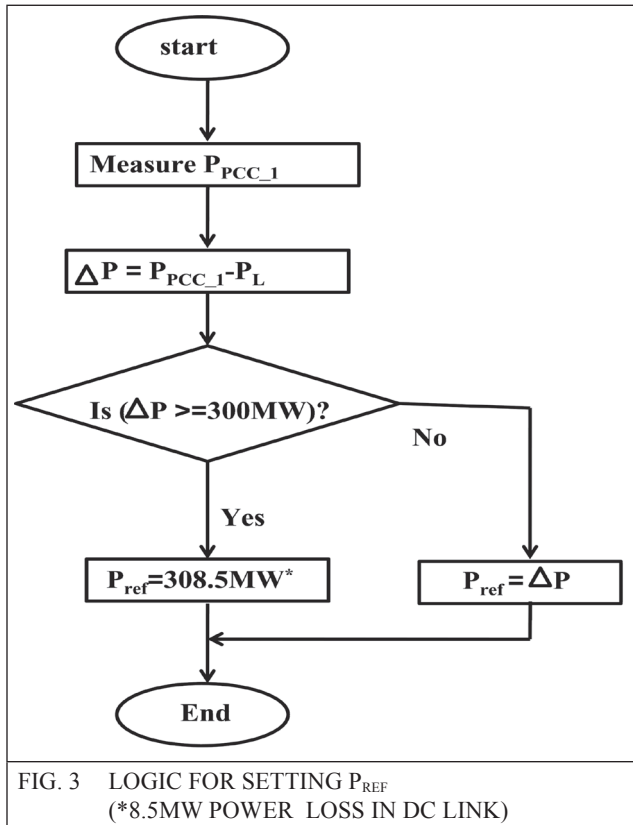
2.3 Reactive power controller

The reactive power (Q_{ac}) is expressed in d and q components of the voltage and current [15], and is given by equation (7). In steady state, $v_{sq} = 0$ and hence, Q_{ac} is given by equation (8).

$$Q_{ac}(t) = \frac{3}{2} [-v_{sd}(t)i_{sq}(t) + v_{sq}(t)i_{sd}(t)] \quad \dots(7)$$

$$Q_{ac}(t) = \frac{3}{2} [-v_{sd}(t)i_{sq}(t)] \quad \dots(8)$$

$$i_{qref} = -\frac{2Q_{ref}}{3v_{sd}} \quad \dots(9)$$



2.4 DC voltage controller

An accurate DC voltage controller is required at the inverter input terminals to maintain a constant DC voltage for different power generating conditions in AC system-1 of Figure 2. In this controller, the reference DC link voltage, which is equal to 300 kV is compared with the measured DC voltage at the inverter input terminals. The error voltage is given to a PI controller. Symmetrical optimum method has been considered to tune the controllers [16]. The output of the PI controller is the reference i_d component of the current (i_{dref}), and is given to inner current controller as shown in Figure 2.

2.5 AC Voltage controller

This controller is used in the inverter side of the transmission system. As stated earlier, the function of this controller is to maintain the AC voltage in the inverter output at the reference value. In this controller, the voltage across the AC filter on the inverter side (v_{cf}) as shown in Figure 2, is compared with the reference AC voltage, and the error is passed through a PI

controller. The required amount of reactive power (Q_{ref}) to be supplied for maintaining the AC voltage constant at the reference value is derived from this PI controller. The reactive current i_{qref} is derived from Q_{ref} , by using (9). The q component of the AC current i_{sq} tracks i_{qref} . The v_{cf} value is computed using (10):

$$v_{cf} = i_{sq} \left(\frac{1}{C_f s} \right) \quad \dots(10)$$

where C_f is the filter capacitor.

In the following section, different case studies are considered to test the dynamic performance of the system shown in Figure 1.

3.0 SIMULATION RESULTS

Simulation studies have been carried out for the system shown in Figure 1. As shown in the figure,

1. AC system-1 is the IPP's generating station (G with internal impedance Z) with a Short Circuit (SC) level of 2000 MVA and a local load that is equal to 10% of generated power connected at PCC-1.
2. AC system-2 is grid substation of agency granting permission for setting up of the generating station, with SC level of 10000 MVA.
3. An AC transmission line (AC line-1) is connected between PCC-1 and PCC-3, to which central grid is connected with a SC level of 12000 MVA.
4. PCC-2 and PCC-3 are interconnected through another AC line (AC line-2).

The complete system data is provided in Table 1. The proposed VSC-HVDC system is designed for a maximum active power transmission of 300 MW.

In the following section two case studies are considered and the steady state performance analysis is carried out for the system shown in Figure 1. The results are presented based on

- i) System parameters
- ii) Controller parameters.

TABLE 1

SYSTEM DATA

SYSTEM DATA	
AC system-1	L-L voltage: 220kV, 50Hz, 2000MVA equivalent Local load: 10% of power generated, 220 kV, 0.85 lag
AC system-2	Equivalent AC source representing state grid substation with a SC level of 10000MVA L-L voltage : 220 kV, 50 Hz
Central Grid	Equivalent AC source representing central grid substation with a SC level of 12000 MVA L-L voltage : 220 kV, 50 Hz
Converter transformer	315 MVA, 50 Hz Winding 1 : Y connected, 220 kV(L-L rms), Resistance:0.002pu, Leakage reactance:0.08pu Winding 2 : Δ connected, 150 kV(L-L rms), Resistance:0.002pu, Leakage reactance:0.08pu
DC transmission line	$R=0.04242 \Omega / \text{km}$ (ACSR Bersimis conductor of diameter 35mm) length=100 km
DC link and Reactor	DC voltage: $\pm 150 \text{ kV}$, Rated Power: 300 MW, DC capacitor: 70 μF Reactor inductance = 0.034 H, Reactor resistance = 0.10 Ω
AC Transmission line	Zebra conductors with positive and zero sequence resistance of 0.0746 Ω/km and 0.219 Ω/km respectively, positive and

	zero sequence inductance of 0.0012 H/km and 0.004 H/km respectively, positive and zero sequence capacitances of 9.34e-009 F/km and 5.86e-009 F/km respectively. Line length=100 km
Filter parameters	1. Double tuned filter for 5th and 7th harmonics: 15 MVAR 2. Single tuned for 27th harmonic: 18 MVAR 3. Single tuned for 54th harmonic: 22 MVAR

3.1 Case studies

3.1.1 Results based on system parameters:

Case i) Generated power in AC system-1 is less than 330 MW

To simulate this condition, the load angle of G in AC system-1 of Figure 1 is set to -5° to generate 220 MW of power. The local load at PCC-1 for this developed power is 22 MW. It is found from Figure 4 that, the system reaches steady state at around 0.04 secs. The power at PCC-1 ($P_{\text{PCC-1}}$) is around 220 MW. Out of this, around 22 MW is supplied to the local load of AC system-1 (P_L) and remaining power of around 198 MW is transmitted through the DC link (P_{dc}) as seen from Figure 4(b) and (c). Also from the Figure 4(d), it is observed that, the power through AC line-1 ($P_{\text{ac line-1}}$) is zero. The power flow into state grid (P_{acgrid}) during this period is approximately 356 MW, which is the sum of DC link power (around 191 MW) and the power through AC line-2, $P_{\text{ac line-2}}$ (around 175 MW).

Case ii) Generated power in AC system-1 is equal to 330MW

To simulate this condition, the load angle of G is changed to -1° at 0.8sec to generate 330 MW of power. The local load at PCC-1 is changed to 33

MW. As observed from Figure 4(b), P_L is found to be around 33 MW and P_{dc} is found to be little less than 300 MW (around 297 MW). Since the power at PCC-1 is just sufficient to supply the local load and DC line power, the AC line-1 power is zero. P_{acgrid} during this period is approximately 460 MW, which is the sum of DC link power (around 298 MW) and the power through AC line-2 (around 172 MW). It is seen from Figure 4 that, the power at PCC-1 and power in the AC transmission lines is subjected to oscillations before reaching a steady state value at around 0.85 sec, which may be due to change in the load angle of G.

Case iii) Generated power in AC system-1 is equal to installed capacity

To simulate this condition, the load angle of G is changed to 16° to generate 550 MW of power. The local load at PCC-1 is changed to 55 MW.

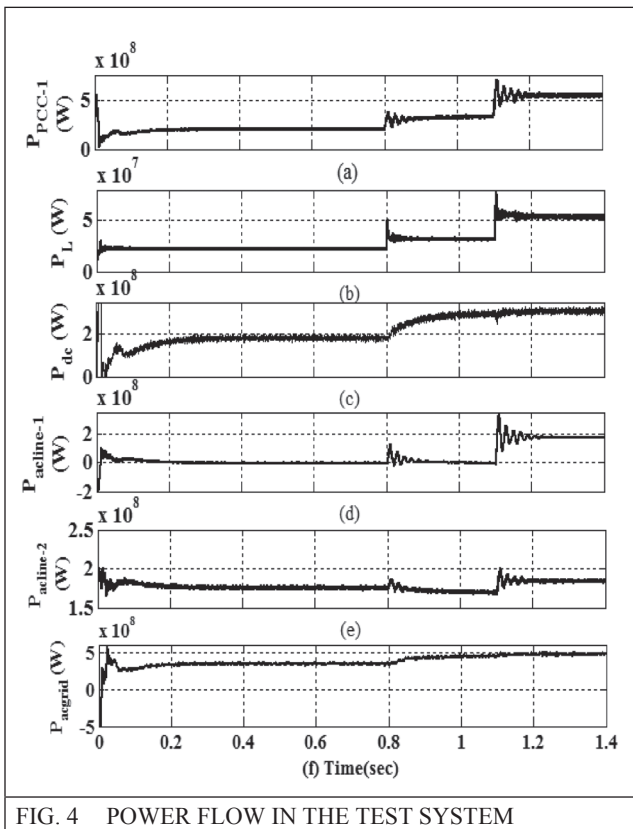


FIG. 4 POWER FLOW IN THE TEST SYSTEM

As observed from Figure 4(b), P_L is found to be 55MW and P_{dc} is found to be 300 MW, the rated power of DC transmission line. $P_{ac line-1}$ is around 182MW with subject to oscillations before reaching a steady state at around 1.2 sec. P_{acgrid}

during this period is approximately 482 MW, which is the sum of P_{dc} (around 300 MW) and $P_{ac line-2}$ (around 182 MW). In this case, even though P_{PCC-1} is 550 MW, the active power controller restricts the power flow in the DC line to 300 MW. The power flow in the various lines shown in Figure 4 is justified due to the load angles at different PCCs as shown in Figure 5(a) and Figure 5(b). The load angles at different buses in the system are tabulated in Table 2. The following equations are satisfied for power flow in different lines.

$$P_{PCC-1} = P_{ac line-1} + P_L + P_{DC} \quad \dots(11)$$

$$P_{ac grid} = P_{DC} + P_{ac line-2} \quad \dots(12)$$

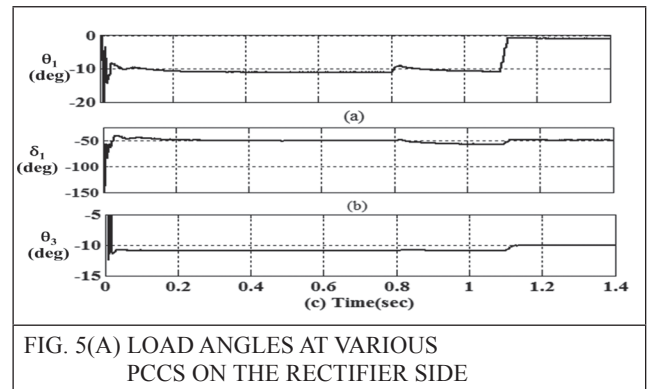


FIG. 5(A) LOAD ANGLES AT VARIOUS PCCS ON THE RECTIFIER SIDE

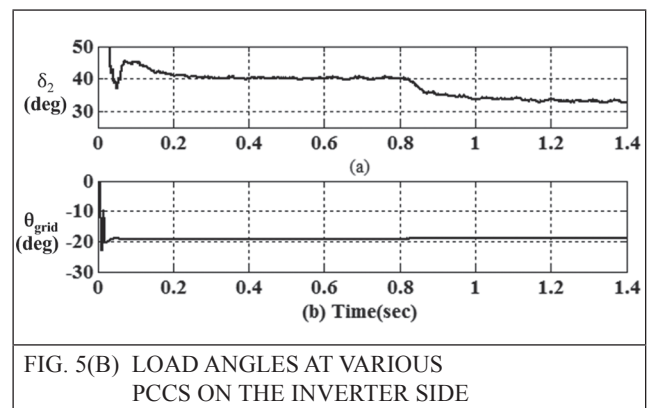


FIG. 5(B) LOAD ANGLES AT VARIOUS PCCS ON THE INVERTER SIDE

TABLE 2			
LOAD ANGLES AT VARIOUS PCCS/ CONVERTER TERMINALS			
PCCs/Converter terminals	Load angle (degrees)		
	During 0 to 0.8 sec	During 0.8 to 1.1 sec	>1.1 sec
Rectifier side:			
At PCC-1(θ_1)	-11	-10	-1
At t1(δ_1)	-50	-57	-50
At PCC-3(θ_3)	-11	-10.75	-10
Inverter side:			
At t2 (δ_2)	40	33	33
At state AC grid (θ_{grid})	-19.25	-18.75	-18.75

Figure 6 shows the DC link voltage, DC link current and the measured DC link power waveforms. As observed from Figure 6(b) and 6(c), for any variation in the DC link power (which is equal to $V_{dc} I_{dc}$), I_{dc} varies, as V_{dc} is constant. The time taken for the DC current to settle at steady state value is almost the same as the time taken for DC power to attain steady state. The reactive power requirement at the rectifier and inverter of VSC-HVDC system is shown in Figure 7. As indicated in the waveform, the reactive power requirement is around -48 MVAR and -44 MVAR for rectifier and inverter. These aspects are considered while designing the AC filters. For the system under consideration, the reactive power requirement is found to be nearly equal to 15 to 16% of the rated DC power of the VSC-HVDC link.

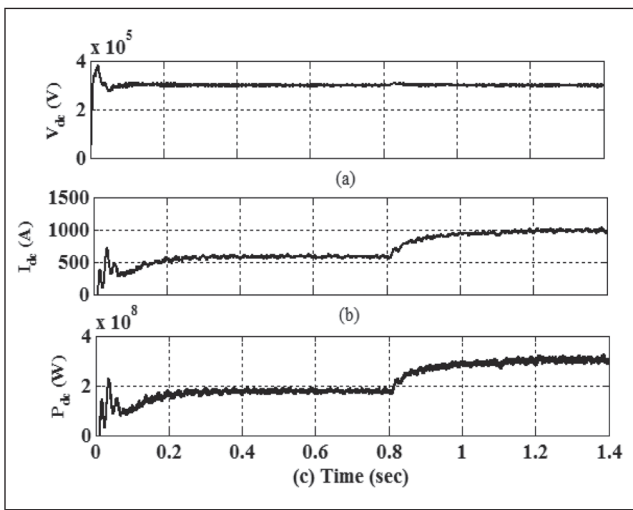


FIG. 6 DC LINK VOLTAGE, CURRENT AND POWER

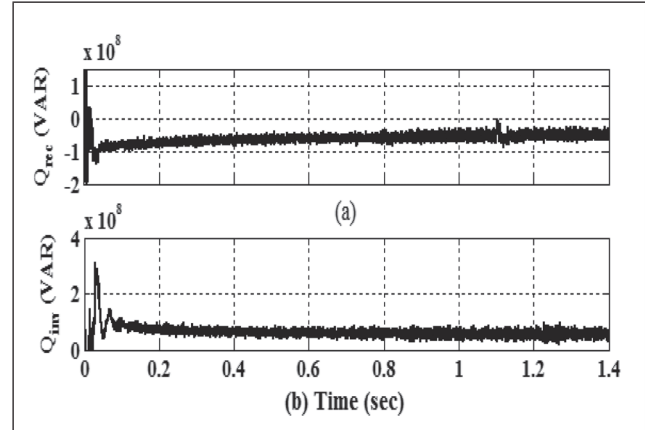


FIG. 7 REACTIVE POWER ON RECTIFIER AND INVERTER SIDE OF VSC-HVDC

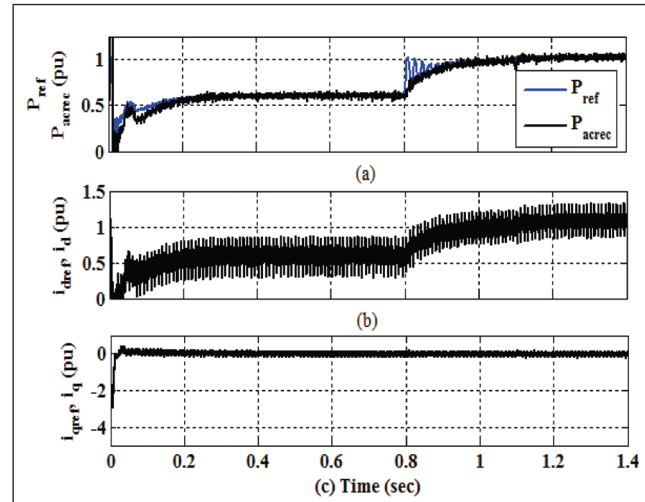


FIG. 8 VSC-1 CONTROLLER PERFORMANCE

3.1.2 Results based on controller parameters:

Figure 8(a) shows the Active power controller performance. Up to 0.8sec, the P_{PCC-1} is less than 330MW as explained in section 3.1.1. Hence, the reference power P_{ref} is less than 1pu. Beyond 0.8 sec, P_{PCC-1} is greater than 330MW. But the reference power is set to a constant value of 1pu. The ac power into the rectifier (P_{acrec}) takes nearly 0.08sec to track P_{ref} . The dynamic power controller outputs the reference i_d current (i_{dref}). From Figure 8(b), it is seen that, i_d tracks i_{dref} almost instantaneously. i_{qref} is set to zero and as seen from Figure 8(c), i_q tracks i_{qref} . It is also observed that, i_d and i_q are independent of each other. Increase in i_d at 0.8 sec has almost no effect on i_q . The DC voltage controller performance is shown in Figure 9(a). The DC link voltage tracks

V_{dcref} in 0.07sec. The change in power at PCC-1 at 0.8sec and 1.1sec has no effect on the DC link voltage. Hence, the DC voltage controller performs well under the situations considered for the studies. i_{dref} and i_d of the inverter current controller are shown in Figure 9(b). i_d tracks i_{dref} almost instantaneously. i_{dref} , derived from DC voltage controller is changing from -0.5 to -0.9pu at 0.8sec. But as observed from Figure 9(a), the DC voltage controller output is constant. The justification for the same is as follows:

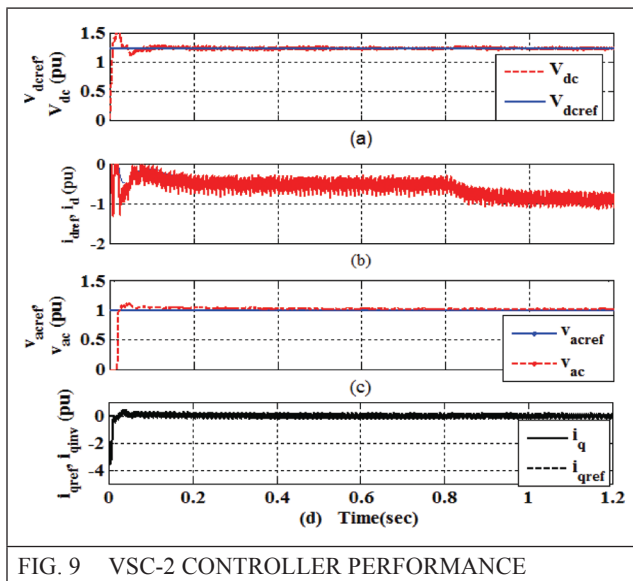


FIG. 9 VSC-2 CONTROLLER PERFORMANCE

The inverter side power is given by (6). Since the converter loss is negligible,

$P_{dc} = P_{ac}(t)$. Hence,

$$P_{dc} = V_{dc}I_{dc} = \frac{3}{2}[v_{sd}(t)i_{sd}(t)] \quad \dots(13)$$

V_{dc} and v_{sd} are held constant due to DC voltage and AC voltage controllers in the inverter station. But, I_{dc} increases at 0.8sec as shown in Figure 8(b). Hence there is change in i_{dref} .

The inverter output voltage is held constant at 1 pu as shown in Figure 9(c), which is due to the robust performance of the AC voltage controller. i_{qref} is derived from AC voltage controller, and as seen from Figure 9(d), it is constant for the entire simulation time. i_q , almost tracks i_{qref} instantaneously.

4.0 CONCLUSION

In this paper, a novel Dynamic power controller for a VSC-HVDC line for power evacuation from an IPP is proposed. The efficient working of the controllers under steady state is illustrated through different case studies for various levels of generated power. The results of the simulation study show that the novel controller proposed in this paper is effective in meeting the DC line transmission constraint imposed by the permitting agency under varying generation levels. From the analysis, it can be concluded that, VSC-HVDC is a promising technology for power evacuation with good control over the power transmitted through the AC line connected to the same PCC.

REFERENCES

- [1] Peter Sandeberg, Lars Stendus, “Large scale Offshore Wind Power Energy evacuation by HVDC Light®”, EWEC 2008, March 31st –April 3rd 2008, Brussels, Belgium.
- [2] L. Kirschner, D. Retzmann, G. Thumm, “Benefits of FACTS for Power System Enhancement”, in IEEE/PES T&D Conference, Dalian – China, 2005.
- [3] D. Ettrich, A. Krummholz, D. Retzmann, K.Uecker, “Prospects of HVDC & FACTS for Bulk Power Transmission and System Security”, in Electrical Networks International Exhibition and Seminar, Moscow – Russia, 2007.
- [4] D. Retzmann, “Global Prospects of Bulk Power Transmission”, in Utility Automation & Engineering T&D, United States of America, 2008.
- [5] It’s time to connect-Technical description of HVDC Light technology, ABB Power Technologies AB, 2006, (<http://www.abb.com/hvdc>)
- [6] Jiuping Pan, Reynaldo Nuqui, Le Tang and Per Holmberg, “VSC-HVDC Control and Application in Meshed AC Networks”, 2008 IEEE-PES General meeting, Pittsburgh, Pennsylvania, July 20-24, 2008.

- [7] Jiuping Pan, Reynaldo Nuqui, Kailash Srivastava, Tomas Jonsson, Per Holmberg, Ying-Jiang Hafner, "AC Grid with Embedded VSC-HVDC for Secure and Efficient Power Delivery", IEEE Energy 2030, Atlanta, GA USA, 17-19 November, 2008.
- [8] Lidong Zhang, Lennart Harnfors, Pablo Rey, "Power System Reliability and Transfer Capability Improvement by VSC-HVDC (HVDC Light)", Security and reliability of electric power systems, CIGRE Regional Meeting, June 18-20, 2007, Tallinn, Estonia.
- [9] Hui Ding, Yi Zhang, Aniruddha M. Gole, Dennis A. Woodford, Min Xiao Han, and Xiang Ning Xiao, "Analysis of Coupling Effects on Overhead VSC-HVDC Transmission Lines From AC Lines With Shared Right of Way", IEEE Trans. Power Delivery, VOL. 25, NO. 4, OCTOBER 2010
- [10] Yan Liu and Zhe Chen, "A Flexible Power Control Method of VSC-HVDC Link for the Enhancement of Effective Short-Circuit Ratio in a Hybrid Multi-Infeed HVDC System", IEEE Trans. Power Systems, VOL. 28, NO. 2, MAY 2013
- [11] Chunyi Guo, Yi Zhang, Aniruddha M. Gole, Chengyong Zhao, "Analysis of Dual – Infeed HVDC with LCC-HVDC and VSC-HVDC", IEEE Trans. Power Delivery, Vol. 27, NO. 3, July 2012.
- [12] Â. J. J. Rezek, C. A. D. Coelho, J. M. E. Vicente, J. A. Cortez, P. R. Laurentino, "The Modulus Optimum (MO) Method Applied to Voltage Regulation Systems: Modeling, Tuning and Implementation", Proc. International Conference on Power System Transients, IPST'01, 24-28 June 2001, Rio de Janeiro, Brazil.
- [13] S. Preitl, R.-E. Precup, "An Extension of Tuning Relations after symmetrical Optimum Method for PI and PID Controllers", Automatica, Vol. 35, 1999, pp 1731-1736.
- [14] M. Machaba, M. Braae, "Explicit Damping Factor Specification in Symmetrical Optimum Tuning of PI Controllers", Proc. of First African Control Conference, 3-5 Des. Cape Town, South Africa, pp.399-404.
- [15] Amirsen Yazdani, Reza Iravani, "Voltage Source Converters in Power systems Modeling, Control and applications", Wiley, IEEE press. p 218-219.
- [16] Chandra Bhajracharya, Marta Molinas, Jon Are Suul, Tore M Undeland, "Understanding of tuning techniques of converter controllers for VSC-HVDC". NORPIE/2008, Nordic Workshop on Power and Industrial Electronics, June 9-11, 2008.